Relativistic mean-field dynamics of giant resonances

Dario Vretenar
Physics Department, University of Zagreb, Croatia

Models based on quantum hadrodynamics provide a consistent description of the nuclear many-body system in terms of interacting baryons and mesons. In the self-consistent mean-field approximation, the time-dependent model has been applied in the analysis of the dynamics of giant resonances. The calculated excitation energies and transition densities of isoscalar giant monopole resonances, restrict the allowed values for the nuclear matter compression modulus $K_{\rm nm}$ to 250–270 MeV. For isoscalar quadrupole and isovector dipole oscillations, evidence is found for modes which can be interpreted as double resonances and which, in a quantized theory, correspond to two-phonon states. The mean-field dynamics of isoscalar and isovector giant resonances displays a transition from order to chaos. Information-theoretic functionals have been used to identify and quantify the nonlinear dynamics in finite nuclear systems that have spatial as well as temporal structure.

Introduction

Relativistic mean-field models provide a microscopically consistent, and yet simple and economical description of the nuclear many-body problem. By adjusting just a few model parameters: coupling constants and effective masses, to global properties of simple, spherical and stable nuclei, it has been possible to describe in detail a variety of nuclear structure phenomena over the whole periodic table, from light nuclei to superheavy elements. When also pairing correlations are included in the self-consistent Hartree-Bogoliubov framework, the relativistic mean-field theory can be applied to the physics of exotic nuclei at the drip-lines. The theory presents a phenomenological description of the nuclear system, and it is based on very simple concepts: (1) nucleons are described as point particles, (2) these particles strictly obey the rules of relativity and causality, and (3) they move independently in mean fields which originate from the nucleon-nucleon interaction. The conditions of causality and Lorentz invariance impose that the interaction is mediated by the exchange of point-like effective mesons, which couple to the nucleons at local vertices. The model parameters are the meson masses and their coupling constants. The essential point in the relativistic description of nuclear structure is the saturation mechanism, which results from the difference between the scalar and the vector densities. For the large components of the Dirac spinors there is an approximate cancelation of the scalar attraction by the vector repulsion. The addition of the scalar and vector potentials for the small components results in large energy splitting between spin-orbit partners.

In the present work we review the applications of time-dependent relativistic mean-field theory to the dynamics of collective vibrations in spherical nuclei. The most elementary collective modes, giant resonances, are highly collective nuclear excitations in which a large fraction of nucleons participate. They can be described as damped harmonic/anharmonic density oscillations around the equilibrium ground-state. Giant resonances occur over the whole periodic table and their characteristic parameters are smooth functions of the mass number. A time dependent mean-field model, therefore, provides a natural framework for the description of the dynamics of small and large amplitude collective motion in nuclei.

The relativistic mean-field model

In theoretical models based on quantum hadrodynamics[1] the nuclear system is described in terms of interacting baryons and mesons. In comparison with conventional non relativistic descriptions, relativistic models explicitly include mesonic degrees of freedom and consider the nucleons as Dirac particles. A variety of nuclear phenomena have been described in the relativistic framework: nuclear matter, properties of finite spherical and deformed nuclei, hypernuclei, neutron stars, nucleon-nucleus and electron-nucleus scattering, relativistic heavy-ion collisions. In particular, relativistic models based on the mean-field approximation have been successfully applied in the description of properties of spherical and deformed β-stable nuclei,[2] and more recently in studies of exotic nuclei far from the valley of beta stability.[3]

The nucleus is described as a system of Dirac nucleons which interact through the exchange of virtual mesons and photons. The Lagrangian density of the model reads

$$\begin{aligned}\mathcal{L} = & \bar{\psi}\left(i\gamma\cdot\partial - m\right)\psi \;+\; \frac{1}{2}(\partial\sigma)^2 - U(\sigma) \\ & - \frac{1}{4}\Omega_{\mu\nu}\Omega^{\mu\nu} + \frac{1}{2}m_\omega^2\omega^2 \;-\; \frac{1}{4}\vec{\mathrm{R}}_{\mu\nu}\vec{\mathrm{R}}^{\mu\nu} + \frac{1}{2}m_\rho^2\vec{\rho}^{\,2} \\ & - \frac{1}{4}\mathrm{F}_{\mu\nu}\mathrm{F}^{\mu\nu} - \; g_\sigma\bar{\psi}\sigma\psi \;-\; g_\omega\bar{\psi}\gamma\cdot\omega\psi \\ & - g_\rho\bar{\psi}\gamma\cdot\vec{\rho}\vec{\tau}\psi \;-\; e\bar{\psi}\gamma\cdot A\frac{(1-\tau_3)}{2}\psi\,. \end{aligned} \tag{1}$$

The Dirac spinor ψ denotes the nucleon with mass m. m_σ, m_ω, and m_ρ are the masses of the σ-meson, the ω-meson, and the ρ-meson, and g_σ, g_ω, and g_ρ are the corresponding coupling constants for the mesons to the nucleon. $U(\sigma)$ denotes the nonlinear σ self-interaction,

$$U(\sigma) \;=\; \frac{1}{2}m_\sigma^2\sigma^2 + \frac{1}{3}g_2\sigma^3 + \frac{1}{4}g_3\sigma^4 \tag{2}$$

and $\Omega^{\mu\nu}$, $\vec{R}^{\mu\nu}$, and $F^{\mu\nu}$ are field tensors. The coupled equations of motion are derived from the Lagrangian density Eq. (1). The Dirac equation for the nucleons:

$$i\partial_t\psi_i = \left[\boldsymbol{\alpha}\left(-i\boldsymbol{\nabla} - g_\omega\boldsymbol{\omega} - g_\rho\vec{\tau}\vec{\boldsymbol{\rho}} - e\frac{(1-\tau_3)}{2}\boldsymbol{A}\right)\right.$$

$$+\beta(m+g_\sigma\sigma)+g_\omega\omega_0+g_\rho\vec{\tau}\vec{\rho}_0+e\frac{(1-\tau_3)}{2}A_0\Big]\psi_i \quad (3)$$

and the Klein-Gordon equations for the mesons:

$$\left(\partial_t^2-\Delta+m_\sigma^2\right)\sigma=-g_\sigma\rho_s-g_2\sigma^2-g_3\sigma^3, \quad (4)$$
$$\left(\partial_t^2-\Delta+m_\omega^2\right)\omega_\mu=\ g_\omega j_\mu, \quad (5)$$
$$\left(\partial_t^2-\Delta+m_\rho^2\right)\vec{\rho}_\mu=\ g_\rho\vec{j}_\mu, \quad (6)$$
$$\left(\partial_t^2-\Delta\right)A_\mu=\ ej_\mu^{\rm em}. \quad (7)$$

In the relativistic mean-field approximation, the nucleons described by single-particle spinors ψ_i are assumed to form the A-particle Slater determinant $|\Phi\rangle$, and to move independently in the classical meson fields. The sources of the fields, i.e. densities and currents, are calculated in the *no-sea* approximation:[4,5]
—the scalar density

$$\rho_{\rm s}\ =\ \sum_{i=1}^{A}\bar{\psi}_i\psi_i, \quad (8)$$

—the isoscalar baryon current

$$j^\mu\ =\ \sum_{i=1}^{A}\bar{\psi}_i\gamma^\mu\psi_i, \quad (9)$$

—the isovector baryon current

$$\vec{j}^{\,\mu}\ =\ \sum_{i=1}^{A}\bar{\psi}_i\gamma^\mu\vec{\tau}\psi_i, \quad (10)$$

—the electromagnetic current for the photon-field

$$j_{\rm em}^\mu\ =\ \sum_{i=1}^{A}\bar{\psi}_i\gamma^\mu\frac{1-\tau_3}{2}\psi_i-\frac{\kappa_i}{2m}\partial_\nu(\bar{\psi}_i\sigma^{\mu\nu}\psi_i)\ . \quad (11)$$

The summation is over all occupied states in the Slater determinant $|\Phi\rangle$. Negative-energy states do not contribute to the densities in the *no-sea* approximation of the stationary solutions. It is assumed that nucleon single-particle states do not mix isospin.

The ground state of a nucleus is described by the stationary self-consistent solution of the coupled system of Equations (3)–(7), for a given number of nucleons and a set of coupling constants and masses. The solution for the ground state specifies part of the initial conditions for the time-dependent problem. The dynamics of nuclear collective motion is analyzed in the framework of the time-dependent relativistic mean-field model, which represents a relativistic generalization of the time-dependent Hartree-Fock approach. For a given set of initial conditions, i.e. initial values for the densities and currents, the nuclear dynamics is described by the simultaneous evolution of A single- particle Dirac spinors in the time-dependent mean fields. Equations (3)–(7) are equivalent to the equation of motion for the one-body density operator $\hat{\rho}=\hat{\rho}(t)$

$$i\hbar\frac{\partial}{\partial t}\hat{\rho}=[h_D,\hat{\rho}]\,, \quad (12)$$

with an initial condition for $\hat{\rho}$

$$\hat{\rho}(t_{in})=\hat{\rho}_{in}. \quad (13)$$

h_D is the single-nucleon Dirac hamiltonian defined in Eq. (3). Starting from the self-consistent solution that describes the ground-state of the nuclear system, initial conditions are defined to simulate excitations of giant resonances in experiments with electromagnetic or hadron probes. Frequencies of eigenmodes are determined from a Fourier analysis of dynamical quantities. In this microscopic model, self-consistent time-dependent mean-field calculations are performed for multipole excitations. An advantage of the time-dependent approach is that no assumption about the nature of a particular mode of vibrations has to be made. Retardation effects for the meson fields are not included in the model, i.e. the time derivatives ∂_t^2 in the equations of motions for the meson fields are neglected. This is justified by the large masses in the meson propagators causing a short range of the corresponding meson exchange forces. Negative energy contributions are included implicitly in the time-dependent calculation, since the Dirac equation is solved at each step in time for a different basis set.[5] Negative energy components with respect to the original ground-state basis are taken into account automatically, even if at each time step the *no-sea* approximation is applied.

The description of nuclear dynamics as a time-dependent initial-value problem is intrinsically semi-classical, since there is no systematic procedure to derive the initial conditions that characterize the motion of a specific mode of the nuclear system. The theory can be quantized by the requirement that there exist time-periodic solutions of the equations of motion, which give integer multiples of Planck's constant for the classical action along one period.[6] For giant resonances the time-dependence of collective dynamical quantities is actually not periodic, since generally giant resonances are not stationary states of the mean-field Hamiltonian. The coupling of the mean-field to the particle continuum allows for the decay of giant resonances by direct escape of particles. In the limit of small amplitude oscillations, however, the energy obtained from the frequency of the oscillation coincides with the excitation energy of the collective state.

Monopole resonances and nuclear compressibility

The study of isoscalar monopole resonances in nuclei provides an important source of information on the nuclear matter compression modulus $K_{\rm nm}$. This quantity is crucial in the description of properties of nuclei, supernovae explosions, neutron stars, and heavy-ion collisions. In principle the value of $K_{\rm nm}$ can be extracted from experimental energies of isoscalar monopole vibrations in nuclei (giant monopole resonances GMR). However, the complete experimental data set on isoscalar GMR does not limit the range of $K_{\rm nm}$ to better than 200–300 MeV. Microscopic calculations of GMR excitation energies might provide a more reliable approach to the determination of the nuclear matter compression modulus. Modern non-relativistic Hartree-Fock plus RPA calculations, using both Skyrme and Gogny effective interactions, indicate that the value of $K_{\rm nm}$ should be in the range 210–220 MeV.[7,8] In relativistic calculations on the other hand, both time-dependent and constrained RMF results indicate that empirical GMR energies are best reproduced by an effective force with $K_{\rm nm}\approx 250$–270 MeV.

In Ref. 9 we have performed time-dependent and constrained RMF calculations for monopole giant resonances for a number of spherical closed shell nuclei, from ^{16}O to the heavy nucleus ^{208}Pb. In order to excite monopole oscillations in a doubly closed-shell nucleus, the spherical solution for the ground-state has to be initially compressed or radially expanded by scaling the radial coordinate. For the case of isoscalar oscillations the monopole deformations of the proton and neutron densities have the same sign. To excite isovector oscillations, the initial monopole deformation parameters of protons and neutrons must have opposite signs. It should also be emphasized that no assumption about the radial nature of the mode of vibrations is made in the time-dependent calculation. We do not have to assume that the motion is adiabatic, or that the mode corresponds to a scaling of the density. The frequency dependence of dynamical quantities and the transition densities are used to determine the structure of the eigenmodes. The frequency can be simply related to nuclear compressibility only if a single compression mode dominates.

For the effective Lagrangian we have used six parameter sets, which differ mostly by their prediction for $K_{\rm nm}$, but otherwise reproduce reasonably well experimental data on nuclear properties. The idea is to restrict the possible values of the nuclear matter compression modulus, on the basis of the excitation energies of giant monopole states calculated with different effective interactions. In addition to the four non-linear sets NL1, NL3, NL-SH and NL2, we have also included two older linear parameterizations, HS and L1. The sets NL1, NL-SH and NL2 have been extensively used in the description of properties of finite nuclei.[2] The new effective interaction NL3 ($K_{\rm nm} = 271.8$ MeV) bridges the gap between NL1 ($K_{\rm nm} = 211.7$ MeV), and NL-SH ($K_{\rm nm} = 355.0$ MeV). This new parameter set provides an excellent description not only for the properties of stable nuclei, but also for those far from the valley of beta stability.[3] For the interaction NL2 the nuclear matter compressibility modulus is $K_{\rm nm} = 399.2$ MeV. From the energy spectra and transition densities calculated with these effective forces, it has been possible to study the connection between the incompressibility of nuclear matter and the breathing mode energy of spherical nuclei. For the isoscalar mode we have found an almost linear relation between the excitation energy of the monopole resonance and the nuclear matter compression modulus.

Rather than the systematics of monopole resonances over the whole periodic table, for the determination of $K_{\rm nm}$ more relevant are microscopic calculations of excitation energies in selected heavy nuclei. The results of RMF calculations for ^{208}Pb are displayed in Fig. 1: time-dependent monopole moments $\langle r^2(t)\rangle = \frac{1}{A}\langle\Phi(t)|r^2|\Phi(t)\rangle$ and the corresponding Fourier power spectra for the nonlinear effective interactions. As one would expect for a heavy nucleus, there is very little spectral fragmentation and a single mode dominates, at least for NL1 and NL3. The experimental excitation energy 13.7 $\pm$ 0.3 MeV is very close to the frequency of oscillations obtained with the NL3 parameter set: 14.1 MeV. The calculated excitation energy for the NL1 parameter set ($K_{\rm nm} = 211.7$ MeV), is approximately 1 MeV lower than the average experimental value. For the linear effective forces HS ($K_{\rm nm} = 545.0$ MeV) and L1 ($K_{\rm nm} = 626.3$ MeV), the oscillations are more anharmonic and the monopole strength is located well above the experimental GMR energy.

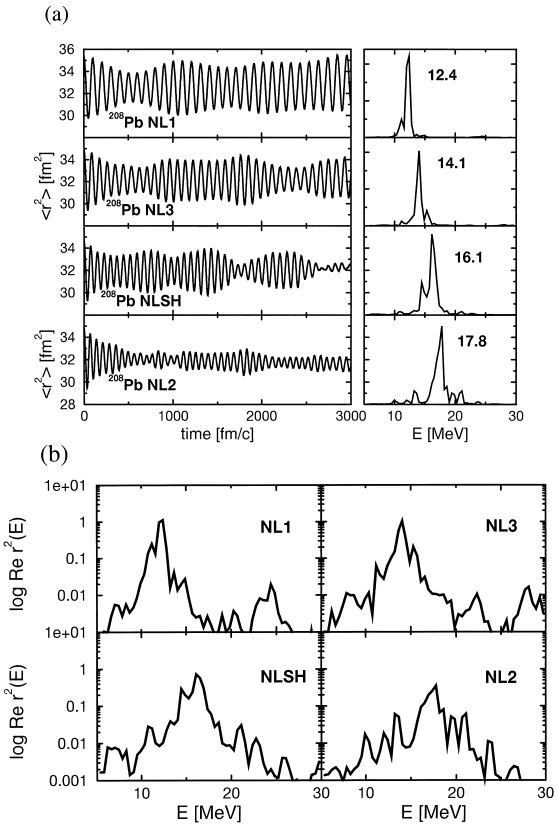

Fig. 1. Time-dependent isoscalar monopole moments $\langle r^2\rangle(t)$ and the corresponding Fourier power spectra for ^{208}Pb. The parameter sets are NL1, NL3, NL-SH and NL2.

In Fig. 2 we display the transition densities that correspond to the main peaks in Fig. 1. It will be useful to separate the volume and surface contributions to the transition densities. We define a velocity field[7]

$$\mathbf{u}(\mathbf{r}) \;=\; -\frac{\mathbf{r}}{r^3\rho_0(r)}\int_0^r r'^2\rho_T(r',E_0)dr' \;, \tag{14}$$

ρ_0 is the ground-state density. $\rho_T(r',E_0)$ denotes the transition density, calculated as the Fourier transform of the time-dependent vector density

$$\rho_B^{p(n)}(r,t) \;=\; \sum_{i=1}^{Z(N)} \psi_i^{+p(n)}(r,t)\psi_i^{p(n)}(r,t). \tag{15}$$

The transition density is separated into two components[7]

$$\rho_T^{\rm vol}(r,E_0) \;=\; \rho_0\boldsymbol{\nabla}\mathbf{u} \;=\; \rho_0\frac{1}{r^2}\frac{d}{dr}(r^2u), \tag{16}$$

$$\rho_T^{\rm surf}(r,E_0) = \mathbf{u}\boldsymbol{\nabla}\rho_0 = u\frac{d\rho_0}{dr}. \tag{17}$$

The resulting volume and surface transition densities are shown in Fig. 2 for all six effective interactions. We notice that the surface contribution does not depend much on the parameter set used, that is, on the nuclear matter incom-

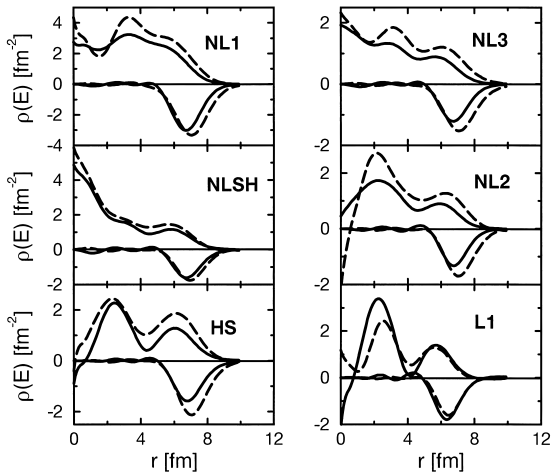

Fig. 2. Volume and surface transition densities for the isoscalar monopole states in ^{208}Pb. Solid lines correspond to proton densities, and dashed lines denote neutron transition densities.

pressibility. The volume transition density, as one would expect, is very sensitive to the value of $K_{\rm nm}$. A very interesting phenomenon is the formation of standing waves in the bulk. It starts already for NL2, but is clearly observed for HS and L1.

The effective interactions NL1 and NL3 seem to produce GMR excitation energies which are quite close to the experimental values. For these two parameter sets we have calculated the isoscalar giant monopole resonances in a number of closed-shell nuclei: ^{40}Ca, ^{56}Ni, ^{100,114,132}Sn, ^{90,122}Zr, ^{146}Gd. The results are shown in Fig. 3. The energies of giant monopole states are determined from the Fourier spectra of the time-dependent monopole moments, and are displayed as function of the mass number. The NL1 excitation energies are systematically lower, but otherwise the two effective interactions produce very similar dependence on the mass number. The empirical curve $E_x \approx 80\ A^{-1/3}$ MeV is also included in the figure, and it follows very closely the excitation energies calculated with the NL3 parameter set. Similar results are obtained from constrained RMF calculations. Both methods indicate that, in the framework of relativistic mean field theory, the nuclear matter compression modulus $K_{\rm nm} \approx 250$–270 MeV is in reasonable agreement with the available data on spherical nuclei. This value is approximately 10–20% larger than the values deduced from recent non-relativistic density dependent Hartree-Fock calculations with Skyrme or Gogny forces. It should be also emphasized that the excitation energy of the isovector monopole resonance in ^{208}Pb, calculated with the NL3 effective force, is in excellent agreement with the experimental value 26 ± 3 MeV.

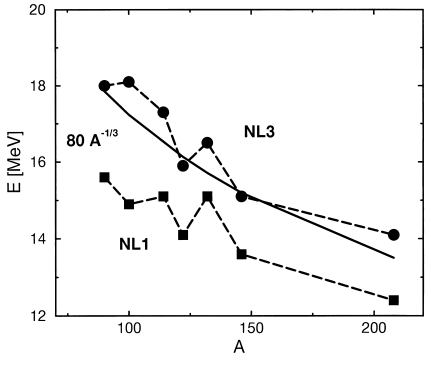

Fig. 3. Excitation energies of isoscalar giant monopole resonances in spherical nuclei as function of the mass number. The effective interactions are: NL1 (squares) and NL3 (circles). The solid curve corresponds to the empirical relation $\approx 80\ A^{-1/3}$ MeV.

Double giant resonances

The physics of giant resonances in nuclei has been the subject of extensive experimental and theoretical studies for many years. However, only recently substantial evidence has been reported for two-phonon states built with giant resonances. Resonant structures that were observed in heavy-ion inelastic scattering, have been interpreted as possible multiple excitations of the giant quadrupole resonance. Double giant dipole resonances have also been discovered in the neutron and in the γ-spectra of nuclei that have been Coulomb excited in relativistic heavy-ion collisions.[10,11] We have performed time-dependent relativistic mean-field calculations and found evidence for modes which can be interpreted as double resonances,[6] and which in a quantized theory correspond to two-phonon states.

As an example of double resonances in light nuclei, we consider the double isoscalar giant quadrupole resonance in ^{40}Ca.[12] The experimental spectrum exhibits a prominent structure, centered at 34 ± 2 MeV excitation energy, with a width of 9 ± 2 MeV. It is interpreted as the two-phonon state of the single isoscalar GQR at 17.5 MeV. Using the NL-SH parameter set for the effective Lagrangian, we have studied isoscalar quadrupole oscillations in ^{40}Ca. The quadrupole mode of oscillations is excited by deforming the spherical solution for the ground-state. For a specific initial deformation, we follow the time-evolution of the collective variable, the quadrupole moment

$$q_{20}(t) = \langle\Phi(t)|\hat{Q}_{20}|\Phi(t)\rangle = \langle\Phi(t)|r^2 Y_{20}|\Phi(t)\rangle. \qquad (18)$$

The time-dependent quadrupole moment shown in Fig. 4 corresponds to an initial axial deformation of the baryon density $\beta = 0.38$. The resulting Fourier spectrum displays a strong peak at 18.5 MeV, in reasonable agreement with the experimental data. We find evidence for excitation of a higher mode

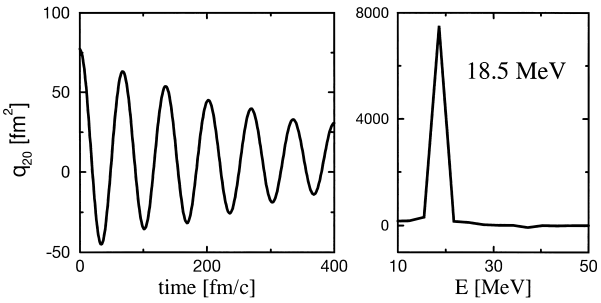

Fig. 4. Time-dependent isoscalar quadrupole moment $q(t)$ and the corresponding Fourier transform for ^{40}Ca. The parameter set is NL-SH, and the initial axial deformation is $\beta = 0.38$.

in the oscillations of the baryon density. The wave function of the nuclear system is a Slater determinant at all times, and therefore can be expanded in the basis of the ground state $|\Phi_0\rangle$

$$|\Phi(t)\rangle = |\Phi_0\rangle + \sum_{mi} z_{mi}(t) a_m^+ a_i \ |\Phi_0\rangle + \sum_{mim'i'} z_{mi}(t) z_{m'i'}(t) a_m^+ a_{m'}^+ a_{i'} a_i \ |\Phi_0\rangle \ + \ ... \tag{19}$$

If the total wave function contains collective $2p$-$2h$ components, they will be observed in the Fourier spectrum of the time-dependent baryon density

$$\rho_B(\mathbf{r},t) \ = \ \sum_{i=1}^{A} \psi_i^+(\mathbf{r},t)\psi_i(\mathbf{r},t). \tag{20}$$

Because of axial symmetry and the isoscalar nature of the excitation, it is sufficient to consider oscillations in time of the baryon density on the positive z-axis. In Fig. 5 we display the

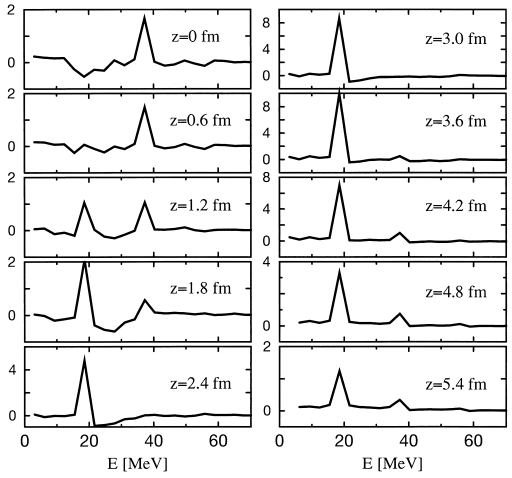

Fig. 5. Fourier transforms of the time-dependent baryon density for various values of the coordinate z, on the axis along which the initial densities are deformed.

Fourier transforms of the time-dependent baryon density for various values of the coordinate z. Two peaks are clearly observed. The first one at 18.5 MeV corresponds to the isoscalar quadrupole resonance. It gradually increases from the center toward the surface of the nucleus. If we plot the values of the Fourier transforms at 18.5 MeV as a function of z, the resulting curve corresponds to the transition density (Fig. 6). The transition density for the first peak is typical for isoscalar quadrupole resonances. The second peak is at 37 MeV, twice the energy of the GQR. It has a maximum in the center of the nucleus, at first decreases with z, but then appears again on the surface. Compared to the GQR transition density, the curve for the 37 MeV peak displays an additional node.

Periodic solutions of the time-dependent Dirac equations can be used to construct the energies of the many-body system. The energy spectrum can be obtained from a semi-classical quantization procedure. One finds periodic solutions such that the mean-field action along a periodic orbit

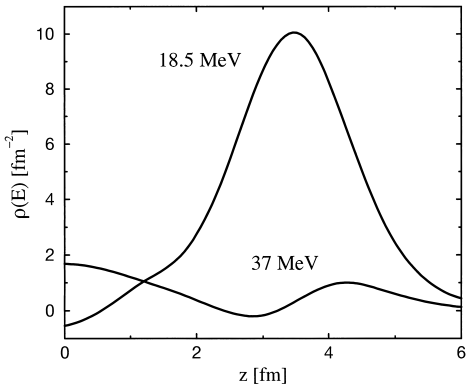

Fig. 6. Isoscalar quadrupole transition densities for the two resonant energies 18.5 and 37 MeV in ^{40}Ca.

$$I \ = \ \sum_i \int_{t_0}^{t_0+T} dt \left[\langle \psi_i(t) | i\hbar \frac{\partial}{\partial t} | \psi_i(t) \rangle \ - \ e_i \right] \tag{21}$$

is equal to an integer multiple of the Planck constant $I = nh$. In Eq. (21) T is the period of oscillations, $|\psi_i(t)\rangle$ denotes time-dependent single-nucleon Dirac spinors, e_i are the corresponding single-nucleon energies in the unperturbed ground-state, and the summation runs over the occupied states. Because of the coupling to the continuum in the mean-field description, giant resonances are not stationary states of the Hamiltonian. Consequently, a non-periodic dependence on time is obtained for dynamical quantities. If the damping is very strong, the giant resonance is not periodic even on the average, and the quantization condition cannot be applied. However, if the motion is nearly periodic, i.e. the damping is relatively weak, the quantization procedure can still be used to calculate the energies, and the effect of damping can be taken into account approximately. In Fig. 7 we display the mean-field action as function of the excitation energy of the nucleons and of the initial deformation β. For the values of β indicated by dots we have integrated the coupled system of Dirac and Klein-Gordon equations and calculated the action integral. The mean-field action is a quadratic function of the initial deformation β, and an almost perfect linear function of the excitation energy. Only above 60 MeV a slight deviation from a pure linear dependence is observed. The values of $\langle E^* \rangle$ for which the action is an integer multiple of the Planck constant are: $I = 1\ h$ for 18.5 MeV, and $I = 2\ h$ for 37.1 MeV.

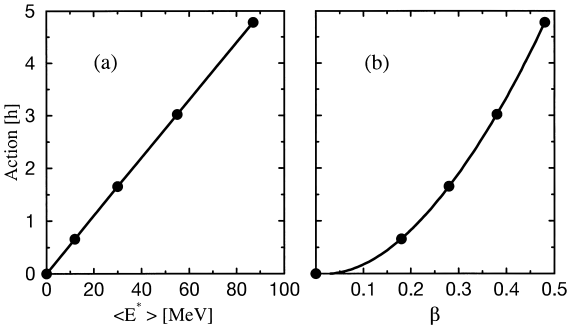

Fig. 7. Mean-field action (21) as function of the excitation energy of the nucleons $E^* = \langle \Phi\ (t)|H_D(t)|\Phi(t)\rangle - \langle \Phi_{GS}|H_D(0)|\Phi_{GS}\rangle$ (a), and of the initial deformation β (b).

Another beautiful example is the double giant dipole resonance that has been observed in relativistic Coulomb excitation of ^{208}Pb.[13] The single GDR is found at 13.3 ± 0.1 MeV with a width of 4.1 ± 0.1 MeV. The sum energy of coincident photon pairs displays a broad structure at 25.6 ± 0.9 MeV with a width of 5.8 ± 1.1 MeV. It is interpreted as the double GDR. In order to excite isovector dipole motion we define the initial conditions: at $t = 0$ (in the center of mass system) all protons start moving in the $+z$ direction with velocity v_π, and all neutrons start moving in the $-z$ direction with velocity $v_\nu = \frac{Z}{N} v_\pi$. For the NL-SH parameter set, the Fourier spectrum of the time-dependent dipole moment displays a strong peak at 12.9 MeV excitation energy, in good agreement with experimental data. We have found that the mean-field action is an integer multiple of the Planck constant: $I = 1\ h$ for $\langle E^* \rangle = 12.9$ MeV, and $I = 2\ h$ for $\langle E^* \rangle = 25.9$ MeV. Therefore, the energy of the one-phonon state, calculated from the mean-field action, coincides with the resonant energy of the mean peak in the Fourier spectrum, and the two-phonon state at 25.9 MeV is in excellent agreement with the experimental value for the excitation energy of the double GDR.

Nonlinear dynamics of giant resonances

Atomic nuclei provide excellent examples of quantum systems in which the transition from regular to chaotic dynamics can be studied. Signatures of chaotic dynamics have been observed in correlations of nuclear level distributions, and in the microscopic and collective motion of the nuclear many-body system. Theoretical studies have shown that regular collective modes coexists with chaotic single-nucleon motion: the adiabatic mean-field created by the nucleons averages out the random components of their motion.

We have analyzed isoscalar and isovector monopole oscillations in spherical nuclei.[14] In Fig. 8 results are shown of time-dependent relativistic mean-field calculations for isoscalar and isovector oscillations in ^{208}Pb. In Fig. 8(a) we plot the time series of the isoscalar monopole moment $\langle r^2(t) \rangle$, and in Fig. 8(b) the corresponding isovector moment $\langle r_{\rm p}^2(t) \rangle -$ $\langle r_{\rm n}^2(t) \rangle$ is displayed. The isoscalar mode displays regular undamped oscillations, while for the isovector mode strongly damped anharmonic oscillations are observed. On the right-hand panels we plot the corresponding Fourier power spectra. The Fourier spectrum of the isovector mode is strongly fragmented, but the main peaks are found in the energy region 25–30 MeV, in agreement with the experimental data. For the isoscalar mode, the time series of the monopole moment and the Fourier spectrum show that the oscillations of the collective coordinate are regular. On the other hand, the appearance of a broad spectrum of frequencies seems to indicate that the isovector oscillations are chaotic. For time-series that result from linear physical processes the Fourier analysis unfolds the characteristic frequencies which are invariants of the dynamics, i.e. they classify the dynamics. For nonlinear systems the corresponding analysis is somewhat more complicated.

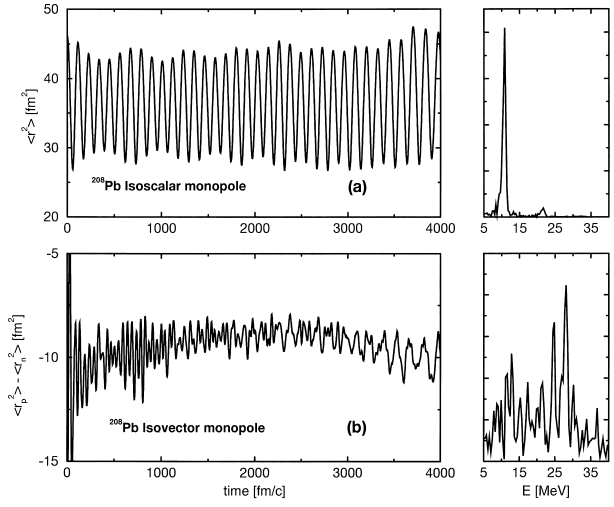

Fig. 8. Time-dependent isoscalar $\langle r^2 \rangle$ (a), and isovector $\langle r_{\rm p}^2 \rangle - \langle r_{\rm n}^2 \rangle$ (b) monopole moments for ^{208}Pb.

We have performed the analysis of the phase spaces reconstructed from time-series of collective dynamical variables that characterize the isoscalar and isovector osci-llations.[15] For the reconstruction of the dynamics two principal quantities have to be determined:[16] the time delay and the dimension of the phase space on which the attractor unfolds. The delays which define the time-lagged variables have been determined from the first minima of the average mutual information functions. This function can be considered as a generalization of the linear autocorrelation to nonlinear systems, and it tells us how much information can be obtained about a measurement at one time, from a measurement taken at another time. For a time series $x(n) = x(t_0 + n\tau_s)$, $n = 0, 1, 2, .$, with the sampling time τ_s, the average mutual information is defined

$$I(T) = \sum_{n=1}^{N} P(x(n), x(n+T)) \times \log_2 \left[\frac{P(x(n), x(n+T))}{P(x(n))P(x(n+T))} \right], \qquad (22)$$

where T is the time-lag. The probability distribution $P(x(n))$ corresponds to the frequency with which any given value of $x(n)$ appears. The joint distribution $P(x(n),\ x(n+T))$ corresponds to the frequency with which a unit box in the $x(n)$ versus $x(n+T)$ plane is occupied. The information functions calculated from the isoscalar and isovector time-series are displayed in Fig. 9. We notice that on the average there is much more mutual information in the isoscalar signal. The prescription is now to choose as time-lag the value for which $I(T)$ displays the first minimum: 27 fm/c for the isoscalar, and 13 fm/c for the isovector mode.

The embedding dimensions have been determined with the method of false nearest neighbors. For each vector in the phase space of dimension d

$$\vec{y}(n) = x(n), x(n+T), ..., x(n+(d-1)T), \qquad (23)$$

we define a nearest neighbor $\vec{y}^{NN}(n)$, in the sense that the Euclidean distance $R_d^2(n)$ between the two vectors is small. In dimension $(d+1)$ the distance between the two vectors is $R_{d+1}^2(n)$. If the two points were nearest neighbors in dimension d, but now we find that $R_{d+1}^2(n)$ is large compared to $R_d^2(n)$, this must be due to the projection from some higher

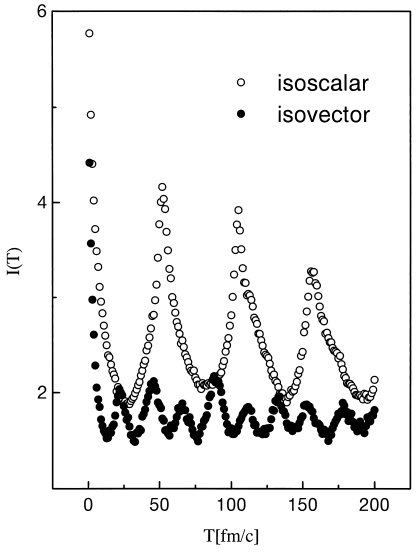

Fig. 9. Average mutual information as a function of time delay for monopole oscillations.

dimensional attractor down to dimension d i.e., they were "false nearest neighbors". The fact that they are found to lie close to each other in dimension d is not a property of the dynamics of the system, but the result of projecting the dynamics onto a phase space of too low dimension. The embedding dimension is now determined from the percentage of nearest neighbors that turn out to be false when going to dimension $(d+1)$. The minimal necessary embedding dimension d_E is the one for which the percentage of false nearest neighbors goes to zero. For the isoscalar and isovector time-series, the false nearest neighbors are displayed in Fig. 10 as functions of the phase space dimension. The percentage of false nearest neighbors goes to zero for $d_E = 3$ (isoscalar mode), and for $d_E = 4$ (isovector mode). These values are taken as embedding dimensions for the reconstruction of the corresponding phase spaces.

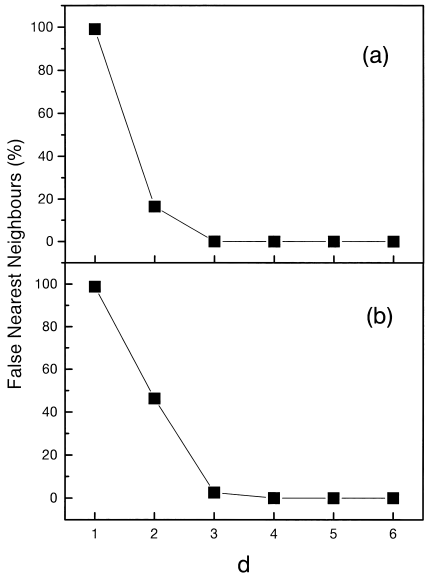

Fig. 10. Percentage of false nearest neighbors as a function of phase space dimension, for isoscalar (a), and isovector (b) modes.

The reconstructed phase space can be represented by the recurrence plot. By embedding the time-series we create a sequence of vectors $\vec{y}(n)$ in the phase space of dimension d_E, and the distance $\delta(m,n) = |\vec{y}(m) - \vec{y}(n)|$ between any two vectors can be calculated. To construct the recurrence plot we choose some distance r, and ask when $|\vec{y}(m) - \vec{y}(n)| < r$. m is placed on the horizontal axis, n on the vertical axis, and a dot is placed at the coordinate (m,n) if $|\vec{y}(m) - \vec{y}(n)| < r$. For a periodic signal the recurrence plot displays a series of stripes at 45 degrees. If a time-series is chaotic, the recurrence plot has a more complicated structure. It is non-uniform and boxes of dense points appear along the diagonal. The recurrence plots for the phase spaces of the isoscalar and isovector time-series are shown in Fig. 11. We notice a pronounced difference between the two modes. For the isoscalar mode the recurrence plot displays a pattern representative for regular oscillations, with stripes separated by a distance that corresponds to the period of oscillations. On the other hand, the recurrence plot for the isovector mode indicates non-stationarity.

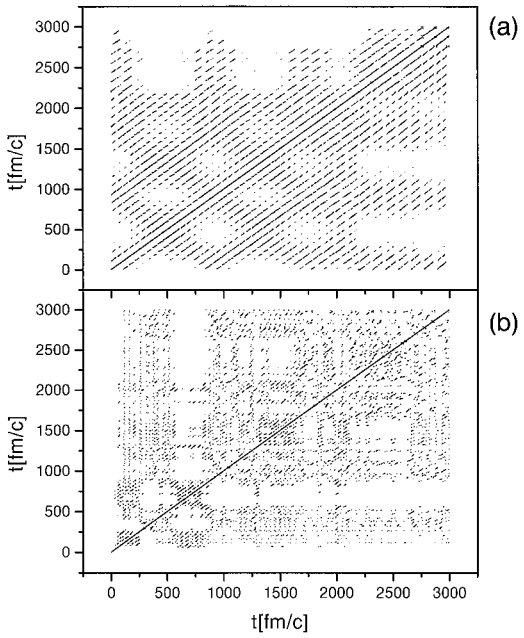

Fig. 11. Recurrence plots for the time-series of isoscalar (a), and isovector (b) monopole oscillations.

If the dynamics of a system is deterministic, the ensemble of phase space trajectories converges towards an invariant subset of the phase space - the attractor. For chaotic dynamics the attractor has fractional dimension, whereas the dimension is integer for regular dynamics. The correlation dimension of the attractor can be numerically evaluated from the correlation integral. If there are N points $\vec{y}(n)$ in the reconstructed phase space of dimension d, we can compute all distances $|\vec{y}(m) - \vec{y}(n)|$. The correlation integral is defined[17)]

$$C_2(r) = \frac{2}{N(N-1)} \sum_{m \neq n}^{N} \Theta(r - |\vec{y}(m) - \vec{y}(n)|), \qquad (24)$$

for a distance r in phase space. $\Theta(x) = 0$ if $x < 0$ and $\Theta(x) = 1$ for $x > 0$. In a certain range of r, the scaling re-

gion, $C_2(r)$ behaves like $C_2(r) = r^d$. The correlation dimension D_2 is determined by the slope of the *log* $C_2(r)$ versus *log* r. It is defined as the slope of the plot in the $r \to 0$ limit. The dimension of the attractor can be determined by plotting *log* $C_2(r)$ versus *log* r for a set of increasing dimensions of the phase space. As the embedding dimension increases, the correlation dimension D_2 should saturate at a value equal to the attractor's correlation dimension. For the isoscalar mode, for $d \geq 3$, we have found that the correlation dimension saturates at $D_2 = 2$. The integer value for the dimension of the attractor indicates regular dynamics. For the isovector mode the correlation dimension does not saturate, but slowly increases to some fractional value between 2 and 3. The fractional dimension of the attractor would imply chaotic or stochastic dynamics.

The identification and quantification of the regular or chaotic dynamics can be also based on the evaluation of information-theoretic functionals. For the time-dependent one-body nucleon densities, we have calculated the von Neumann information entropy functionals[15)]

$$S(t) = -\int \rho(\vec{r},t)\ \log_2\ \rho(\vec{r},t)\ d^3r. \tag{25}$$

The Fourier analysis has shown that the entropy of the isoscalar mode contains the same information as the dynamical variable, but the structure is more complicated for the isovector mode. Collective oscillations of densities with finite spatial extension provide excellent physical examples for the analysis of systems that have spatial as well as temporal structure. For a nonlinear system in chaotic regime, the influence of spatial motion on temporal chaos can be studied: what are the spatial correlations in a finite system that displays chaotic oscillations of a collective dynamical variable? We might consider, for example, the conditional entropy defined from a two-body total density

$$S_2(t) = -\int \rho^2(\vec{r},\vec{r}\,',t) \times \log_2\ \left[\frac{\rho^2(\vec{r},\vec{r}\,',t)}{\rho(\vec{r},t)\rho(\vec{r}\,',t)}\right]\ d^3r\ d^3r', \tag{26}$$

where the two-body density matrix ρ^2 is defined from the Slater determinant of occupied states. The conditional entropy should provide a measure of two-body spatial correlations. The time-dependent entropies Eq. (26) that corresponds to isoscalar and isovector oscillations are shown in Fig. 12. They are compared with the value that results from the time-evolution of the system that has not been excited (time-dependent entropy of the ground state). For the isoscalar mode, regular modulated oscillations are observed. The entropy that corresponds to the isovector mode is much lower and more irregular at the beginning, but it eventually approaches values comparable to those of the isoscalar mode. Similar to the entropy defined on the one-body density operator, this behavior reflects the strong mean-field damping of the isovector oscillations. The information contents of the "two-body" entropies are shown in the corresponding Fourier power spectra in Fig. 13. For the isoscalar mode the entropy contains the same information as the dynamical variable, and there is a high degree of two-body correlations for the isoscalar mode, the nucleon density oscillates with the same frequency at all points in the nuclear system. For the

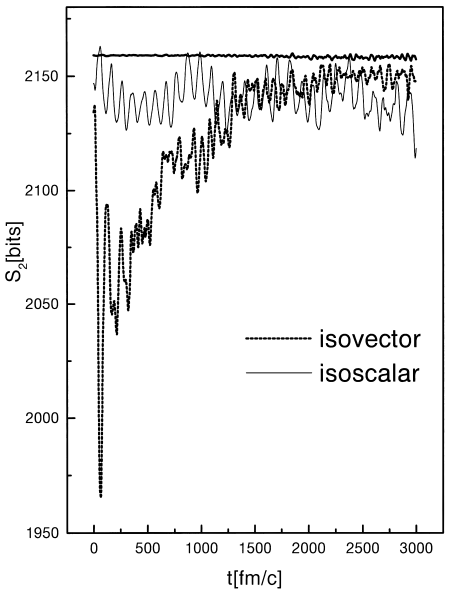

Fig. 12. Time-dependent conditional entropies (26) for isoscalar and isovector monopole motion. The thick solid line is the reference ground-state entropy.

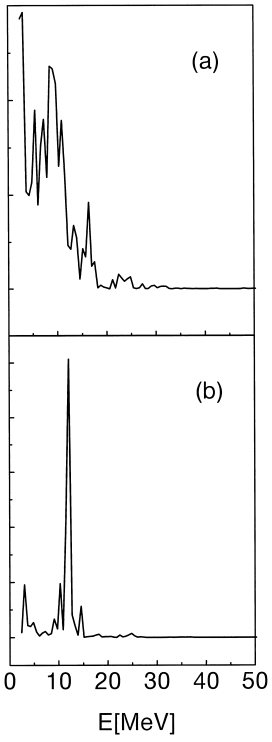

Fig. 13. Fourier power spectra of the conditional entropies (26) for isovector (a), and isoscalar (b) monopole oscillations.

isovector mode no useful information is found in the Fourier spectrum. There is a highly fragmented structure in the region of the isoscalar giant resonance, but in addition strong peaks are observed in the very low frequency region.

In the analysis of isoscalar and isovector oscillations we might ask how much information is contained in the dynamical variable of the neutron distribution, about the proton subsystem,

and vice versa. For a time-series $x(n)$, an information function is defined

$$I_{\pi(\nu)}(\epsilon) = -\sum_i P_i(x_{\pi(\nu)}) \log_2 P_i(x_{\pi(\nu)}). \quad (27)$$

The probability distribution $P_i(x)$ corresponds to the frequency with which any given value of x appears in the box i of dimension ϵ. For two time-series, the corresponding joint information function is

$$I_{\pi,\nu}(\epsilon) = -\sum_{i,j} P_{i,j}(x_\pi, y_\nu) \log_2 P_{i,j}(x_\pi, y_\nu). \quad (28)$$

The joint distribution $P_{i,j}$ corresponds to the frequency with which a box (i,j) (linear dimension ϵ) in the x_π versus y_ν plane is occupied. The average amount of information about the variable y that the variable x contains is quantified by the mutual information

$$M_{x,y}(\epsilon) = I_x(\epsilon) + I_y(\epsilon) - I_{x,y}(\epsilon). \quad (29)$$

Clearly, the mutual information vanishes if $P_{i,j}(x,y) = P_i(x)P_j(y)$, i.e. if x and y are statistically independent.. In our example of giant monopole resonances, the variable x corresponds to the mean square radius of the proton distribution, and y to that of the neutron distribution. The mutual information functions (in units of bits) are displayed in Fig. 14, for the isoscalar and isovector oscillations: the average amount of information that $\langle r^2 \rangle$ of the proton density contains about the dynamical variable of the neutron distribution is more than a factor three larger for the isoscalar mode.

Another interesting possibility is to consider the mutual information as function of the spatial coordinate. Instead of using as dynamical variables integrated quantities like the mean square radii, we can follow the time evolution of the proton and neutron densities at various points along the radial axis. The dynamical variables will be the values of the proton and neutron densities at each point in space, and we can plot the average mutual information of the densities as function of the radial coordinate. The results are shown in Fig. 15 for ^{16}O, ^{40}Ca, and ^{208}Pb. In all three nuclei the mutual information of the proton and neutron density is much higher for the isoscalar mode. In fact, for ^{16}O and ^{40}Ca, the mutual information for the isovector mode practically vanishes, and no radial dependence is observed. The isoscalar mode displays a very interesting radial behavior of the mutual information. It is high in the nuclear volume, but there is also a pronounced minimum at the radius that corresponds to the surface of the nucleus. This means that there is little correlation between proton and neutron densities in the surface region, they oscillate almost independently. The nucleons at the surface are less bound, and the effective compression modulus of the surface region is different from that in the volume of the nucleus. The slowly vibrating self-consistent potentials in which the protons and neutrons move, do not average on the surface in the same way as in the bulk region.

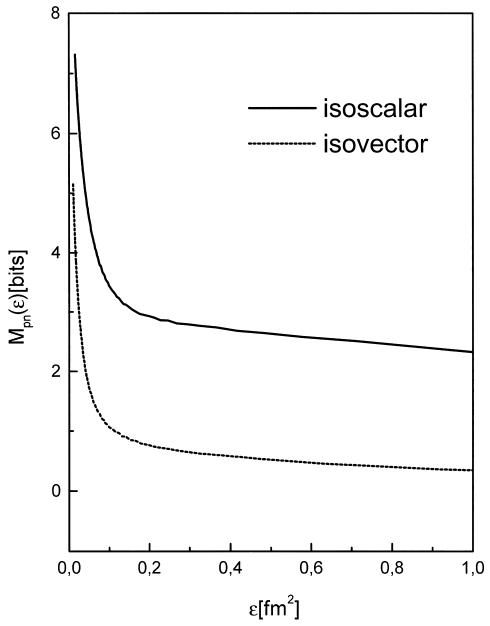

Fig. 14. Mutual information (29) between the time-dependent mean square radii of the proton and neutron density distributions. The two curves that correspond to isoscalar and isovector oscillations, are plotted as functions of the size of the box in the linear embedding of the time-series.

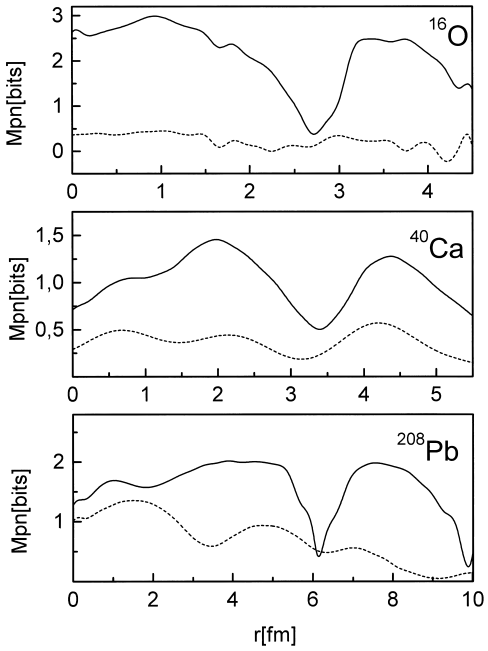

Fig. 15. Radial dependence of the mutual information between proton and neutron density distributions. Results for ^{16}O, ^{40}Ca and ^{208}Pb are displayed. Solid curves correspond to isoscalar oscillations, dashed curves to isovector oscillations.

Summary

A time-dependent version of the relativistic mean-field model has been applied in the analysis of the nonlinear dynamics of nuclear giant resonances. The characteristic properties of these collective excitations vary smoothly with the size of the nucleus, and therefore a self-consistent mean-field approach provides a consistent description of nucleon dynamics. Starting from the self-consistent mean-field solution for the ground

state, and a set of appropriate initial conditions, the full set of time-dependent relativistic mean-field equations is solved, and dynamical variables are analyzed. Collective isoscalar and isovector oscillations are described, which correspond to giant resonances in spherical nuclei. The excitation energies and the structure of eigenmodes are determined from a Fourier analysis of dynamical multipole moments and densities.

The giant monopole resonances of a number of spherical closed shell nuclei, from ^{16}O to the heavy nucleus ^{208}Pb, have been investigated in order to constrain the range of allowed values for the nuclear matter incompressibility. Time-dependent calculations have been performed for several effective interactions with significantly different values of $K_{\rm nm}$. We have found that the effective interactions NL1 and NL3 produce GMR excitation energies which are close to the experimental data. Based on the very precise experimental value for the isoscalar GMR energy in the heavy nucleus ^{208}Pb, which is rather well reproduced by the set NL3, we have derived a value of approximately 250 MeV for the incompressibility of nuclear matter. For a series of doubly closed-shell nuclei, the effective interaction NL3 reproduces the empirical mass dependence $E_x \approx 80\ A^{-1/3}$ MeV. The value $K_{\rm nm} \approx 250$–270 MeV is in reasonable agreement with the available data on spherical nuclei. This value is 10–20% larger than the values deduced from recent non-relativistic density dependent Hartree-Fock calculations with Skyrme or Gogny forces At present the origin of this discrepancy is not fully understood.

Results of model calculation for isoscalar quadrupole and isovector dipole oscillations have been compared with experimental data on giant resonances in ^{40}Ca and ^{208}Pb, respectively. The eigenmodes have been determined from the Fourier spectra of the dynamical variables, i.e. time-dependent quadrupole and dipole moments. We have found a very good agreement between the calculated frequencies of oscillations and the experimental excitation energies of isoscalar GQR in ^{40}Ca and isovector GDR in ^{208}Pb. For both these modes experimental data on double giant resonances have been reported recently, consistent with the harmonic oscillator picture. We have studied possible excitations of higher modes which can be interpreted as double resonances, and which, in a quantized theory, correspond to two-phonon states. For the isoscalar quadrupole oscillations in ^{40}Ca, we find evidence for a higher mode in the Fourier spectra of the time-dependent baryon density. The energy spectra of isoscalar quadrupole and isovector dipole oscillations have also been determined from the requirement that the mean-field action, calculated along a periodic orbit, is an integer multiple of the Planck constant. In both cases an excellent agreement is obtained between the energies of one-phonon states and the resonant energies of the peaks in the Fourier spectra of time-dependent quadrupole and dipole moments. The calculations predict essentially harmonic spectra, both for ^{40}Ca and ^{208}Pb, in agreement with available experimental data. In particular, for ^{208}Pb, the calculated energies of one- and two-phonon states are in excellent agreement with data on single and double GDR. Deviations from pure harmonic spectra are small and well above the excitation energies that correspond to two-phonon states.

Giant resonances provide excellent examples for the study of regular and chaotic dynamics in quantum systems. In addition, the finite spatial extension of nuclei enables the analysis of spatio-temporal behavior in nonlinear dynamical systems. The nucleons move in the effective self-consistent single particle potentials, and the equations of motion describe the time evolution of the one-body density. Since the time-dependent potentials are calculated in a self-consistent way, the model of the nuclear system is intrinsically nonlinear, and chaotic motion is expected for specific initial conditions. From the time-series of isoscalar and isovector monopole moments of ^{208}Pb, we have reconstructed the corresponding phase spaces. The analysis of the resulting recurrence plots and correlation dimensions indicates regular motion for the isoscalar mode, and chaotic dynamics for the isovector oscillations. The nonlinear dynamics of giant resonances has also been analyzed in the framework of information-theoretic functionals. For the time-dependent one-body nucleon densities, we have calculated the von Neumann information entropy functionals. The spatial correlations have been described with a time-dependent conditional entropy defined from a two-body nucleon density. From the average mutual proton-neutron information function, we have shown that the information which is contained in the collective dynamical variable of the proton density, about the neutron density, is large for the isoscalar mode and it practically vanishes for the isovector oscillations. Finally, the mutual information between proton and neutron densities has also been analyzed as a function of the spatial coordinate. It has been observed that this function displays an interesting radial dependence, which reflects the differences in the dynamics of the monopole vibration in the volume and on the surface of the nucleus.

References

1) B. D. Serot and J. D. Walecka: Adv. Nucl. Phys. **16**, 1 (1986); Int. J. Mod. Phys. E **6**, 515 (1997).
2) P. Ring: Progr. Part. Nucl. Phys. **37**, 193 (1996).
3) D. Vretenar, P. Ring, and G. A. Lalazissis: in *Proc. Nuclear Structure '98*, edited by C. Baktash (Am. Inst. Phys. New York, 1999), in press.
4) D. Vretenar, H. Berghammer, and P. Ring: Phys. Lett. B **319**, 29 (1993).
5) D. Vretenar, H. Berghammer, and P. Ring: Nucl. Phys. A **581**, 679 (1995).
6) P. Ring, D. Vretenar, and B. Podobnik: Nucl. Phys. A **598**, 107 (1996).
7) J. P. Blaizot: Phys. Rep. **64**, 171 (1980).
8) J. P. Blaizot, J. F. Berger, J. Dechargé, and M. Girod: Nucl. Phys. A **591**, 435 (1995).
9) D. Vretenar, G. A. Lalazissis, R. Behnsch, W. Pöschl, and P. Ring: Nucl. Phys. A **621**, 853 (1997).
10) H. Emling: Progr. Part. Nucl. Phys. **33**, 729 (1994).
11) T. Aumann, P. F. Bortignon, and H. Emling: Annu. Rev. Nucl. Part. Sci. **48**, 1 (1998).
12) J. A. Scarpaci et al.: Phys. Rev. Lett. **71**, 3766 (1993).
13) J. Ritman et al.: Phys. Rev. Lett. **70**, 53 (1993).
14) D. Vretenar, P. Ring, G. A. Lalazissis, and W. Pöschl: Phys. Rev. E **56**, 6418 (1997).
15) D. Vretenar, N. Paar, P. Ring, and G. A. Lalazissis: Phys. Rev. E **59**, 6418 (1999).
16) H. D. I. Abarbanel, R. Brown, J. J. Sidorowich, and L. Sh. Tsimring: Rev. Mod. Phys. **65**, 1331 (1993).
17) P. Grassberger and I. Procaccia: Phys. Rev. Lett. **50**, 346 (1983).